

Article

Prediction of Seasonal Frost Heave Behavior in Unsaturated Soil in Northeastern China Using Interactive Factor Analysis with Split-Plot Experiments and GRNN

Hanli Wan ^{1,2} , Jianmin Bian ^{1,2,*}, Juanjuan Wu ^{1,2}, Xiaoqing Sun ^{1,2}, Yu Wang ^{1,2} and Zhuo Jia ^{1,2}

¹ College of New Energy and Environment, Jilin University, Changchun 130021, China

² Key Laboratory of Groundwater Resources and Environment, Ministry of Education, Jilin University, Changchun 130021, China

* Correspondence: bianjm@jlu.edu.cn; Tel.: +86-1800-431-9968

Received: 16 May 2019; Accepted: 29 July 2019; Published: 31 July 2019



Abstract: Few studies of frost heave mechanisms have considered multifactor interactions, particularly in unsaturated saline soils typical of northeastern China. We collected soil samples in western Jilin Province and assessed their potential frost heave behavior with reference to four controllable factors: soluble salt content (CSS), compactness (C), temperature (T), and water content (WC) using a two-level split-plot experiment. The resulting frost heave ratio was between -0.6% and 2.1% . Analysis of variance showed that water content, compactness, and temperature had significant effects on frost heave behavior, with water content having the strongest correlation (factor coefficient of 0.82), while content of soluble salt (CSS) had no significant effect. The interaction factors (products of single factors) $CSS \times WC$ and $C \times WC$ had significant effects on frost heave behavior. A correlation analysis using these interaction factors with experimental data drawn from previous research showed results consistent with the improved frost heave experiment as the significant effects of single factors on frost heave behavior ranked from $WC > C > T$ and the interaction factors $CSS \times WC$ and $C \times WC$ gain had significant effects. We then established two generalized regression neural network (GRNN) models based on the single and interaction factors in order to predict frost heave behavior, showing that adding the latter to the input dataset improved the model accuracy. Thus, future research on predicting frost heave behavior in unsaturated saline soils should consider multiple interacting factor for greater accuracy.

Keywords: frost-heaving; interaction factors; split-plot experiment; unsaturated saline soil; GRNN

1. Introduction

Frozen soil can be divided into permafrost, seasonal frozen soil, and short-term frozen soil [1]. In cold regions, freeze damage caused by frozen soils seriously threatens ecological functions and engineering safety. Unsaturated soil is widely distributed in cold regions; when the temperature drops below the freezing point, the water in such soil begins to freeze [2]. During this process, soil water, vapor, and heat move from warm to cold locations, driven by a complicated process involving the temperature gradient and soil water potential. At the same time, discontinuous ice lens growth in the unsaturated soil causes frost-heaving [3–5], leading to soil body expansion and uneven uplift of the ground surface [6]. This process can cause serious damage to above-ground and underground infrastructure, resulting in serious economic losses [1,7,8]. For example, uplift and cracking of road surfaces or changes in railway grades can threaten safe transportation [9] or disrupt buried pipes

and cables. The study of frost heave mechanisms began in 1961, when Everett [10] proposed the first theoretical basis for this process. This was followed by further research proposing many mathematical models [11–14], further defining frost heaving as hydrothermal coupling and migration manifested as the growth of ice lens bodies in the soil [13,15,16]. However, few studies have focused specifically on frost heaving in unsaturated soils, making further research on the mechanisms of frost heave behavior in unsaturated soil and analyses of influential factors of great significance for the prevention and control of frost damage in cold regions.

Frost heaving is affected by many factors, including soil characteristics and external environmental factors. For example, the proportion of fine-grained (clay and silt) content in soil has a significant effect: lower levels are correlated with less frost heaving [3,10]. The amount of water content also directly affects frost heaving, while highly saline soils will produce salt expansion at low temperatures [17–19]. The compactness, temperature gradient, and depth to groundwater table are additional factors affecting this process [20,21]. Most frost heave experiments have focused on investigating the effects of single factors [19–22] using the one-factor-at-a-time (OFAT) experimental approach, in which tests are conducted by systematically changing the levels of one single factor while holding the levels of all other factors fixed. This approach is not capable of considering possible interactions between multiple factors and is less efficient than other methods based on a statistical approach [23].

Design of Experiments (DOE) is a defined approach to developing valid experimental designs, scientifically analyzing test data, and observing changes in response (dependent variables) by adjusting the level of controllable factors (independent variables) [23,24]. Unlike OFAT, factors in DOE are varied together. DOE is often used for multifactorial experiments in which the analysis of experimental data can determine the impact of single factors on the response while identifying interactions between different factors. One example is the split-plot experiment design, first proposed by Fisher in 1925, has great advantages in cost, efficiency, and validity [25,26]. In addition, this approach allows the definition of hard-to-change (HTC) factors, whose levels are difficult to adjust or will increase experimental cost. We applied this approach in the current study to account for the many interacting factors influencing frost heave while considering the fact that some factors (such as compactness and salt content) are difficult to randomize. Moreover, neural network models based on biological neural network systems are widely used in civil engineering and engineering geology, including the back propagation neural network (BPNN) and generalized regression neural network (GRNN). Of these, the latter has higher error tolerance and stronger ability to solve nonlinear problems [27]. As a few studies have applied neural networks to predict the frost heave behavior of saline soil in western Jilin Province, China [20], we used GRNN to predict the frost heave behavior of unsaturated saline soil in this region.

We designed a two-level multifactorial split-plot frost heave experiment and used previously published experimental data [22] with local soil samples to (1) analyze the relationships between frost heave behavior and the soil's soluble salt content, compactness, temperature, and water content; (2) consider the influence and significance of interacting factors on frost heave; and (3) apply two types of GRNN models to predict the frost heave behavior of unsaturated saline soil while assessing the influence of interacting factors on model performance. Our methods and results are of great significance to improved understanding of frost heave mechanisms, predictions of frost heave behavior in saline soil, and prevention and control of freeze damage in the study area. Figure 1 shows the technology route process of this study.

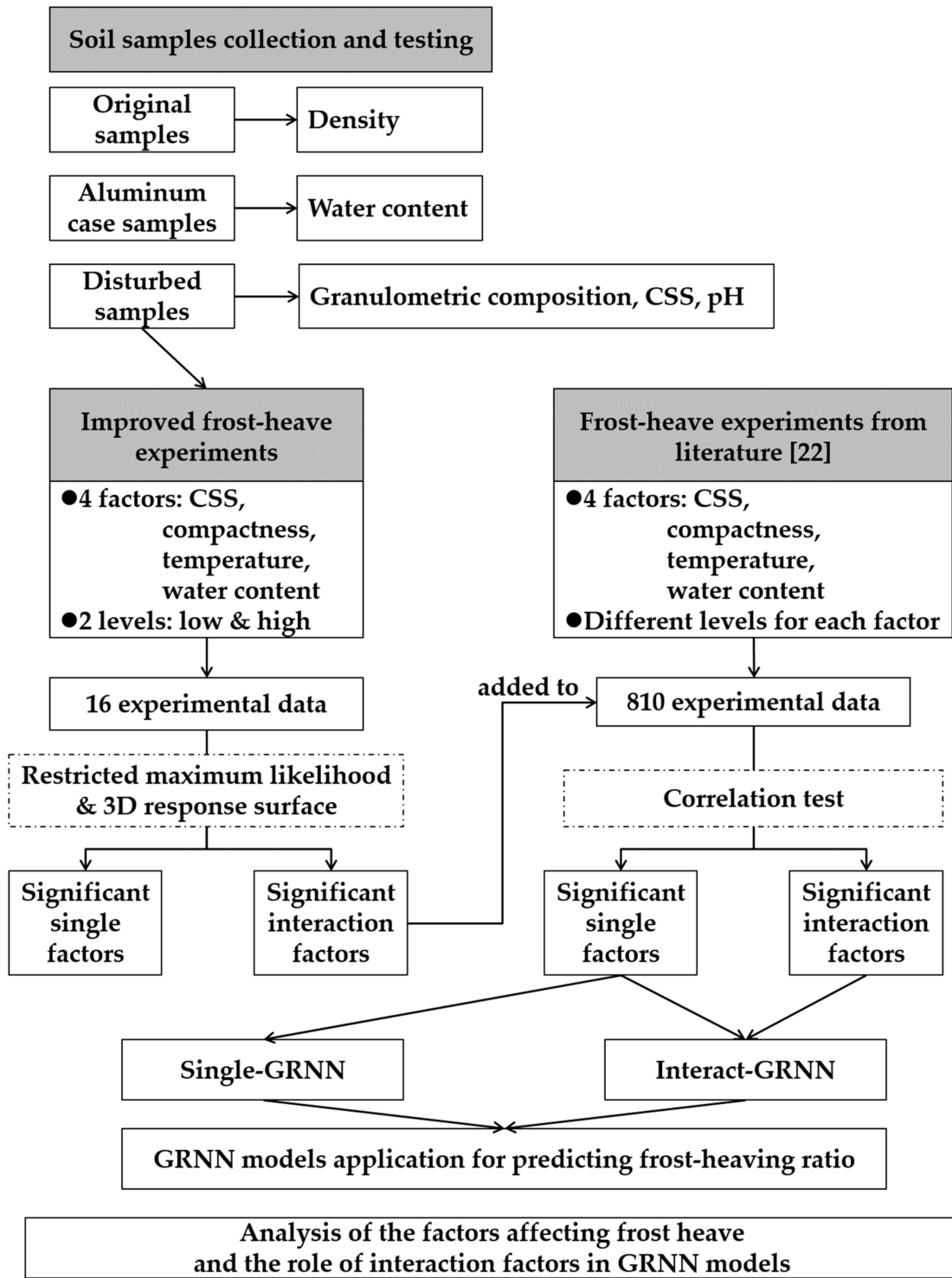


Figure 1. Technology route map of the study process.

2. Materials and Methods

2.1. Study Area

Northeast China experiences large-scale seasonal freezing and is widely characterized by saline soils [28]. The study area in western Jilin Province has a climate that is dry and windy in spring, hot in summer, and cold in winter. Evaporation tends to be far greater than precipitation, resulting in salt accumulation at the soil’s surface. Daily mean temperatures range from 38 °C to −36.5 °C with an

annual average temperature of 4.6 °C. The frozen soil period lasts from November to March, with freeze depth reaching 80–100 cm. As the saline soil begins to form a frozen soil layer, the soil water moves from the unfrozen layer to the frozen layer under the influence of total water potential, carrying solutes to the surface and exacerbating soil salinization [29]. Increased water content at the soil's surface promotes more intense frost heave with associated risks to infrastructure.

2.2. Soil Sample Collection and Testing

2.2.1. Sample Collection

The saline soil used in the experiment was collected from Da'an city in western Jilin Province during May 2009. Soil samples from different depths (20, 30, 40, 50, 70, 100 cm) were collected at a single sampling point using the cutting ring method ($\Phi 100$). As the disturbed soil samples would inevitably lose water during transportation to the laboratory, small amount (~20–30 g) of original soil (3 samples per layer) were collected in aluminum cases, weighed on-site, and kept sealed; these were used to calculate water content while other original samples were used to test soil density. Disturbed soil samples were also collected at each layer, each weighing at least 1000 g; these were used to test granulometric composition, content of soluble salt (CSS), and pH, as well as conducting the improved frost-heaving experiments. Examples of original and disturbed soil samples are shown in Figure 2.

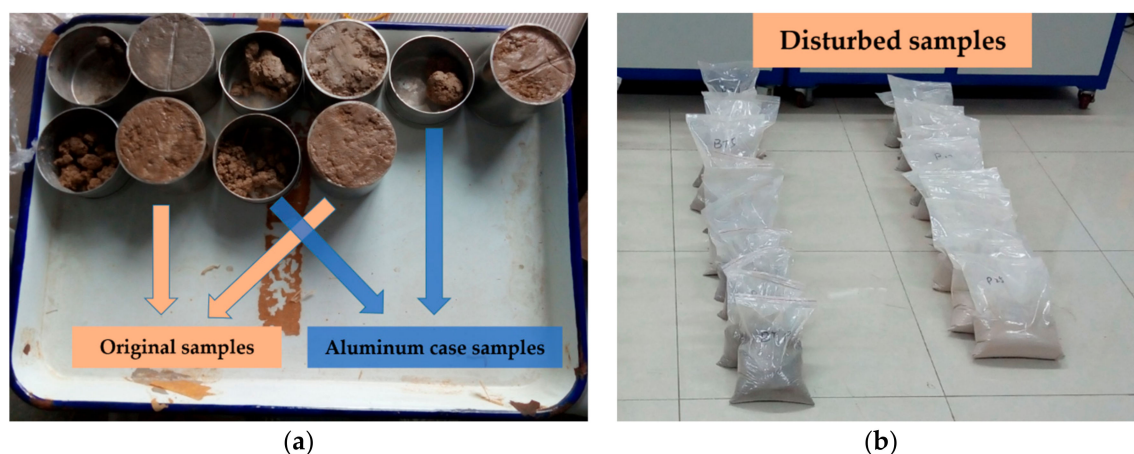


Figure 2. (a) Original and aluminum case soil samples and (b) disturbed soil samples.

2.2.2. Soil Testing

All soil samples were brought back to the laboratory on the same day. Disturbed soil samples were naturally dried, ground, sieved (2 mm), and stored. Granulometric composition, water content, content of soluble salt (CSS), pH, and density were tested at the Key Laboratory of Jilin University. A laser particle size analyzer (Mastersizer 2000) was used to analyze the granulometric composition in terms of clay (<0.002 mm), silt (0.02–0.002 mm), and sand (2–0.02 mm). The remaining indicators were tested following the methods introduced by Bao [30]. All test results are given in Table 1. Water content (density) values are the mean of the 3 original samples for each layer. Granulometric composition, CSS, and pH values reflect the disturbed samples.

Soil samples at different depths clearly had similar granulometric compositions. The fine-grained soil (clay and silt) content values were all high, defining all soil samples as silty clay. Water content was highest at 40, 50, and 70 cm, while the shallowest sample had the lowest water content. The CSS values decreased consistently with depth. As soil with high water content and CSS is most likely to cause serious frost heave activity, we chose to use disturbed soil samples at 30 cm depth for further experimentation.

Table 1. Physical and chemical parameters of the original and disturbed soil samples.

Depths (cm)	Granulometric Composition			Water Content (%)	CSS (%)	pH	Density (g/cm ³)
	Clay (%)	Silt (%)	Sand (%)				
20	31.20	59.20	9.60	12.50	0.60	9.2	1.57
30	41.70	52.80	5.50	19.80	0.55	8.4	1.60
40	36.90	53.60	9.50	20.70	0.49	8.6	1.58
50	44.80	50.60	4.60	20.60	0.35	8.7	1.62
70	43.90	52.00	4.10	20.80	0.28	8.6	1.62
100	42.70	52.70	4.60	18.10	0.29	8.5	1.61

2.3. Experimental Methods

2.3.1. Improved Frost Heave Experiments

Unlike past single-factor studies, our improved frost heave experiments considered interactions between four factors: soluble salt content (CSS), compactness (C), temperature (T), and water content (WC) (Table 2), where the interaction factors are the products of two or three single factors. We used disturbed soil samples at 30 cm depth and determined factor levels with reference to soil properties and experimental data from previous research [22]. CSS was controlled by adding NaHCO₃ to soil samples because the study area was composed of carbonate saline soil. Water content was controlled by adding water [22]. A total of 16 experiments were conducted, divided by temperature conditions (either −25 °C or −4 °C) into two groups that each lasted 12 hours at a fixed temperature (Table 3).

Table 2. Design summary of improved frost heave experiments.

Factors	Name	Change Type ¹	Low Level ²	High Level ²	Code Values ³	
CSS	CSS (%)	Hard	0.5	1.5	−1 = 0.5	1 = 1.5
C	Compactness (%)	Hard	85.0	95.0	−1 = 85.0	1 = 95.0
T	Temperature (°C)	Easy	−25.0	−4.0	−1 = −25.0	1 = −4.0
WC	Water content (%)	Easy	18.0	26.0	−1 = 18.0	1 = 26.0

¹ Change type: The factor is hard to change (HTC) factor or easy to change. ² Low level, high level: Small value of the factor, big value of the factor. ³ Code values: Low (high) level of the factor will be represented by −1 (1) in Design-Expert 10.

Table 3. Schedule and results of improved frost heave experiment.

No.	Factors				Response
	CSS (%)	Compactness (%)	Temperature (°C)	Water Content (%)	η (%)
1	1.5	95.0	−4.0	26.0	1.38
2	1.5	95.0	−25.0	18.0	0.11
3	1.5	85.0	−4.0	18.0	−0.47
4	1.5	85.0	−25.0	26.0	1.93
5	1.5	85.0	−25.0	18.0	−0.60
6	1.5	85.0	−4.0	26.0	1.79
7	1.5	95.0	−25.0	26.0	2.10
8	1.5	95.0	−4.0	18.0	−0.02
9	0.5	85.0	−25.0	26.0	1.43
10	0.5	85.0	−4.0	18.0	−0.23
11	0.5	85.0	−25.0	18.0	−0.23
12	0.5	85.0	−4.0	26.0	1.29
13	0.5	95.0	−25.0	26.0	1.51
14	0.5	95.0	−4.0	18.0	0.54
15	0.5	95.0	−25.0	18.0	0.66
16	0.5	95.0	−4.0	26.0	1.38

Unsaturated soil was placed in an experimental tube with an inner diameter of 5 cm and a height of 10 cm; the soil column height was 8 cm. The tubes were made of thermal insulation material and their bottoms were sealed with the same material to ensure that the soil gradually froze from top to bottom during the experiment, similar to actual natural conditions. A dial indicator was placed above each tube to measure the longitudinal volume change of the soil column (Figure 3).

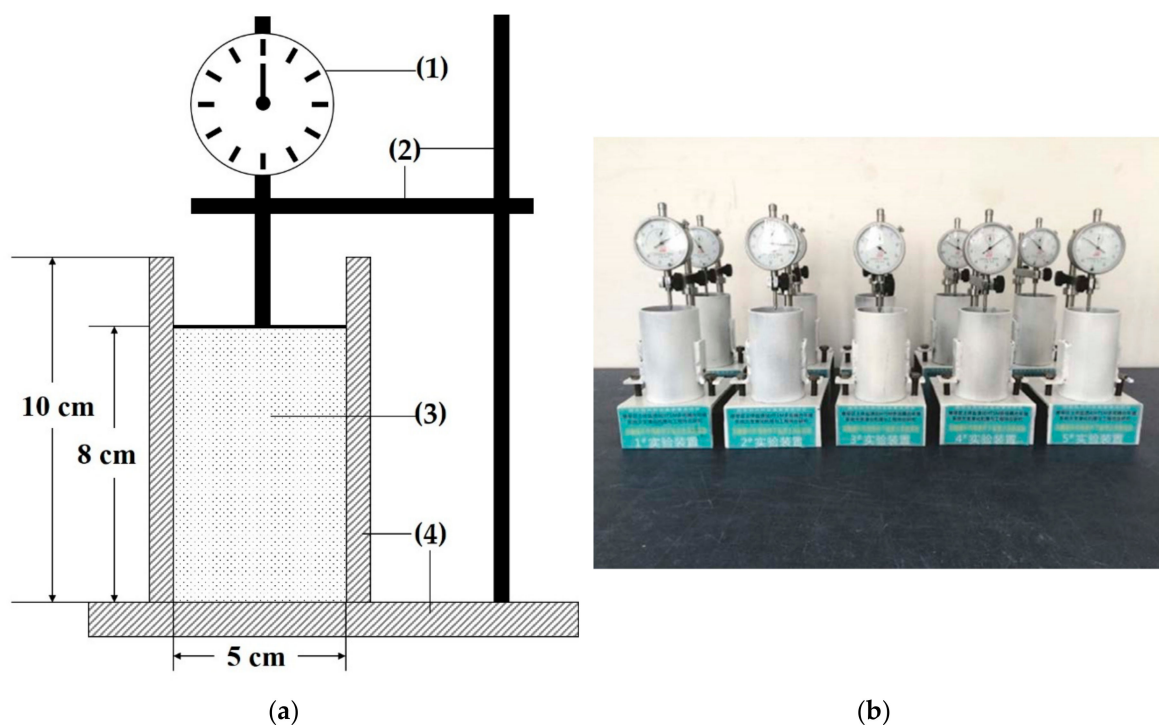


Figure 3. Frost heave experimental setup: (a) schematic showing (1) dial indicator, (2) bracket, (3) soil column, (4) tube and pedestal, and (b) actual apparatus.

The prepared samples were immediately placed in a temperature control box. We defined the frost heave effect η by the following ratio.

$$\eta = \frac{\Delta H}{H_0} \times 100\%, \tag{1}$$

where ΔH (cm) is the height increment of the soil column after freezing and H_0 (cm) is the original height of the soil.

2.3.2. Frost heave Experiments

Bao [22] collected soil samples from the study area and carried out 810 frost heave experiments analyzing the individual influence of same four factors as in our study (Table 4). However, as that study used the OFAT approach, the interactions between these factors could not be determined.

Table 4. Influence levels of four factors in frost heave experiments [22].

Factors	Levels
Compactness (%)	85.0, 90.0, 95.0
CSS (%)	0.0, 0.3, 0.5, 1.2, 1.5
Water content (%)	18.0, 20.0, 21.0, 22.0, 24.0, 26.0
Temperature (°C)	0.0, -2.0, -4.0, -6.0, -8.0, -10.0, -15.0, -22.0, -25.0

2.4. Data Analysis

We conducted all data analysis, including restricted maximum likelihood (REML), *F*-test, data diagnostics, and graphing, using Design-Expert 10 (DX10) [31] software. REML is a method for estimating the parameters of a linear regression model. The *F*-value associated with the regression model is estimated based on the techniques proposed by Kenward and Roger (the KR method) [32]. This method uses the components of variance as estimated by REML, the model being fit, and the design structure to approximate the correct distribution for testing the terms and model subsets. Data diagnostics and graphs can help determine the prediction accuracy of the model (whether predicted values were close to experimental values) [33]. R^2 and adjust- R^2 (Adj- R^2) were used for quantitative assessment of the regression model's prediction accuracy. The former reflects the accuracy of the regression model by showing the degree to which the input variables explain the variation of the output variable. The latter is similar, but also accounts for the number of variables. For the experimental data of Bao [22], we added interaction factors and used correlation analysis between the response (η) and influencing factors.

2.5. Prediction

We used GRNN to predict frost heave behavior using the four influencing factors as input data and the frost heave ratio as the output target. All 810 experimental data points from Bao [22] were randomly divided into 3 groups: a learning dataset (680 data points) for GRNN, a training dataset (100 data points), and a test dataset (30 data points). In order to analyze the influence of interaction factors on the frost heave prediction accuracy, we prepared two types of input datasets: single factors only (Single-GRNN) and single factors with interaction factors CSS×WC and C×WC (Interact-GRNN), using R^2 and root mean square error (RMSE) to evaluate model accuracy. GRNN is a radial basis function neural network proposed by Specht [34] that has a simple training procedure and unique adjustment parameters. The GRNN network structure is divided into four layers (input, pattern, summation, and output; Figure 4). The input vector is $X = [x_1, x_2, \dots, x_m]^T$ and the corresponding output is Y . The dimension of the input vector X is m and the number of samples is n . This model can automatically adjust the network structure according to the training samples; the number of nodes need not be determined by the user.

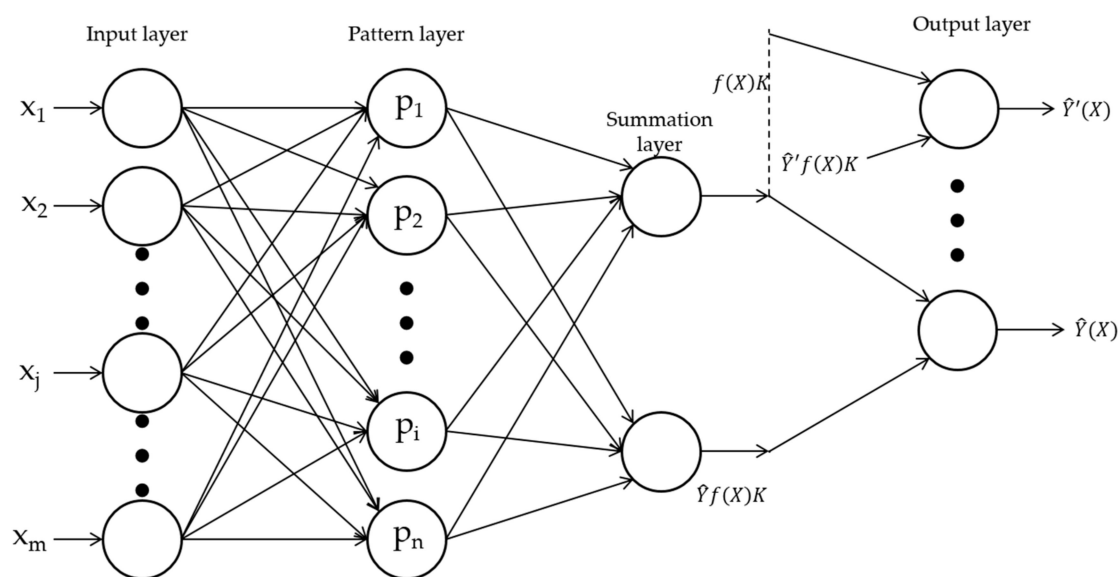


Figure 4. Schematic diagram of generalized regression neural network (GRNN) model structure.

The nodes of input layer are merely distribution nodes, the number of input nodes is equal to the dimension of the input vector, m . Arrows in Figure 3 indicate data input, transfer, and output. The

input layer provides all X to the second layer, the pattern layer. The number of nodes on the pattern layer is equal to the number of samples, n . The activation function is given in Equation (2).

$$p_i = \exp\left[-\frac{[X - X_i]^T [X - X_i]}{2\delta^2}\right], (i = 1, 2, \dots, n) \tag{2}$$

where p_i is the activation function of i -th node, X is the input vector, X_i is the learning sample of i -th node, δ is the smoothing factor, and upscript T means matrix transposition. The pattern layer outputs are passed to the summation layer. Two ways of summation are performed in summation layer. One is $f(X)K$ which is the summation of the outputs of the pattern layer (Equation (3)), the other is $\hat{Y}f(X)K$, which is the summation of the outputs of the pattern layer weighted by the observation output variable Y_i (Equation (4)).

$$f(X)K = \sum_{i=1}^n p_i = \sum_{i=1}^n \exp\left[-\frac{[X - X_i]^T [X - X_i]}{2\delta^2}\right] \tag{3}$$

$$\hat{Y}f(X)K = \sum_{i=1}^n Y_i p_i = \sum_{i=1}^n Y_i \exp\left[-\frac{[X - X_i]^T [X - X_i]}{2\delta^2}\right] \tag{4}$$

where K is a constant that does not need to be computed. The output layer divides $\hat{Y}f(X)K$ by $f(X)K$ to yield the desired estimate of $\hat{Y}(X)$, see Equation (5).

$$\hat{Y}(X) = \frac{\hat{Y}f(X)K}{f(X)K} = \frac{\sum_{i=1}^n Y_i \exp\left[-\frac{[X - X_i]^T [X - X_i]}{2\delta^2}\right]}{\sum_{i=1}^n \exp\left[-\frac{[X - X_i]^T [X - X_i]}{2\delta^2}\right]} \tag{5}$$

3. Results and Discussion

3.1. Results of Improved Frost Heave Experiments

The resulting η values ranged from -0.60% to 2.1% (Table 3). Five of the sixteen response values were negative, indicating that the saline soil shrank rather than swelled under some low-temperature conditions. The coefficient estimates, F -value, and p -value showed that factors compactness, temperature, and water content all had significant effects on η (p -value < 0.05) (Table 5). The effect of CSS on η was not significant, but the interaction factor CSS \times WC had a significant effect on η , indicating that CSS alone had little effect on frost heave behavior but did interact with water content to create an effect. The interaction factor C \times WC also had a significant effect on η .

Table 5. Results coefficient estimates of coded factors, F -value, and p -value.

Factor	DF ¹	Coefficient	F-Value	p-Value
CSS	1	-0.0081	0.084	0.7830
Compactness	1	0.1700	37.79	0.0017*
Temperature	1	-0.0780	7.81	0.0382*
Water content	1	0.8200	851.09	<0.0001*
CSS \times C	1	-0.0570	4.14	0.0976
CSS \times WC	1	0.2100	54.75	0.0007*
C \times T	1	-0.0590	4.51	0.0871
C \times WC	1	-0.1800	41.74	0.0013*
T \times WC	1	-0.0630	5.10	0.0735
CSS \times T \times WC	1	-0.0440	2.52	0.1733

¹ DF: Degrees of Freedom. *: p -value less than 0.05 indicates factors are significant.

Water content had the largest coefficient of interaction (0.82), indicating that the frost heave ratio increased with higher water content; the next-highest factors were CSS × WC (0.21) and C × WC (−0.18). Temperature had the smallest coefficient (−0.078), indicating that frost heave ratio increased only slightly with a decrease in temperature at low-temperature conditions (below 0 °C).

The interactions between CSS and water content, and compactness and water content, are shown in Figure 5, where the two intersecting lines indicate that the effect of one factor depends on the level of the other. The slope of the line can be used to indicate the sensitivity of η to variables. For example, at low CSS (high compactness), η is less sensitive to water content than at high CSS (low compactness). Thus, if we wanted to make the frost heave ratio even more robust to variations in water content, we could reduce CSS (increase compactness).

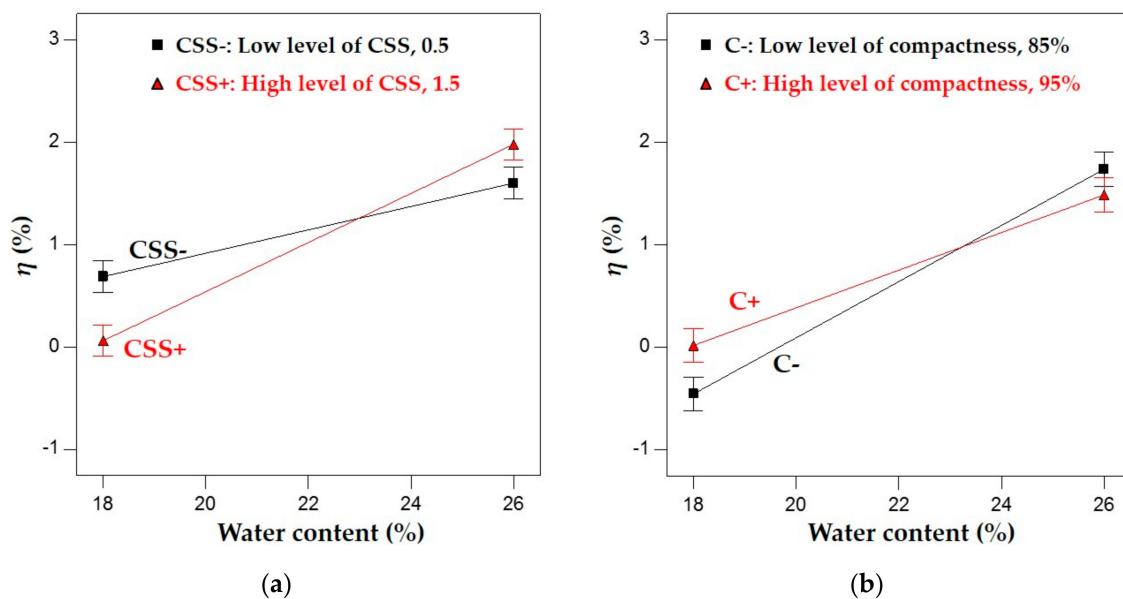


Figure 5. Interaction graphs of (a) soluble salt content (CSS) and water content (b) compactness and water content.

The liner regression model Equation (6) was set up using the factors ranked in descending order of absolute coefficient value (Table 5) to develop the relationship between experimental and predicted results for η (Figure 6). The R² of the model was 0.9951 and the Adj-R² was 0.9754, indicating that the predicted values matched the experimental data.

$$\eta = 0.82 \times WC + 0.21 \times (CSS \times WC) - 0.18 \times (C \times WC) + 0.17 \times C - 0.078 \times T - 0.063 \times (T \times WC) - 0.059 \times (C \times T) - 0.057 \times (CSS \times C) - 0.044 \times (CSS \times T \times WC) - 0.0081 \times CSS + 0.79 \tag{6}$$

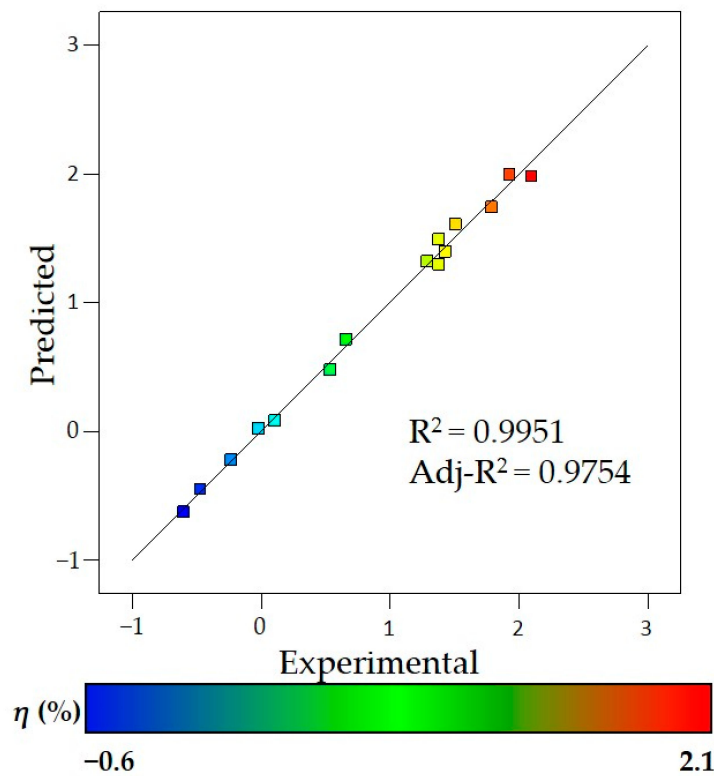


Figure 6. Relationship between experimental and predicted η values, the points are colored by η values and the color is consistent with 3D response surface in Figure 7.

The 3D response surface plots for the effects of CSS and compactness on η at different levels of temperature and water content (Figure 7) show that η had an inverse relationship with temperature, which was most obvious when water content was high (26%) than low (18%). For a given amount of water, lower temperature produced a more complete phase change from liquid to solid such that an increase in ice content can lead to increased η [22]. In contrast, the relationship between η and CSS changed at different water content levels; η increased with increasing CSS when water content was high, but decreased with increasing CSS when water content was low. Compactness and η had a positive relationship when CSS was between $\sim 0.5\text{--}0.7\%$, however when CSS was higher, this effect vanished or even turned inverse. Water content had a clearly positive relationship with η ; when more soil water is available for freezing, more ice lenses form and cause frost-heaving.

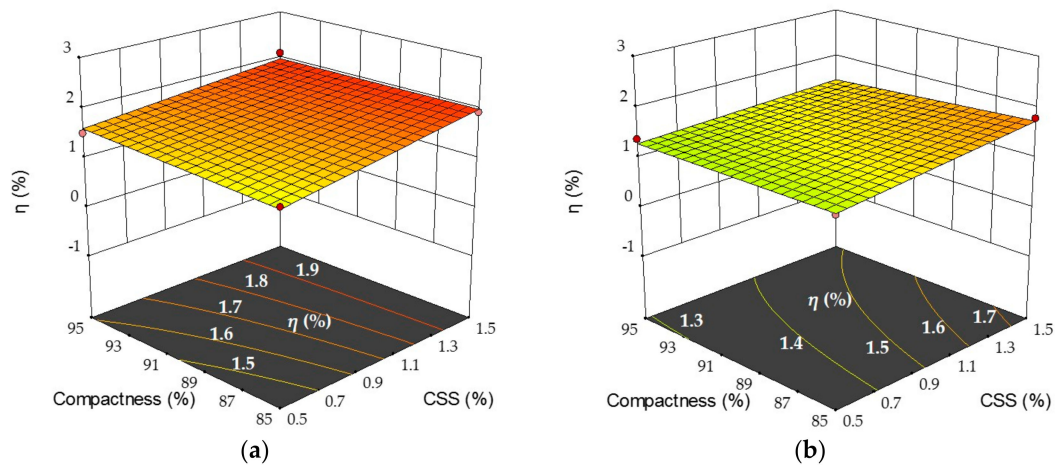


Figure 7. Cont.

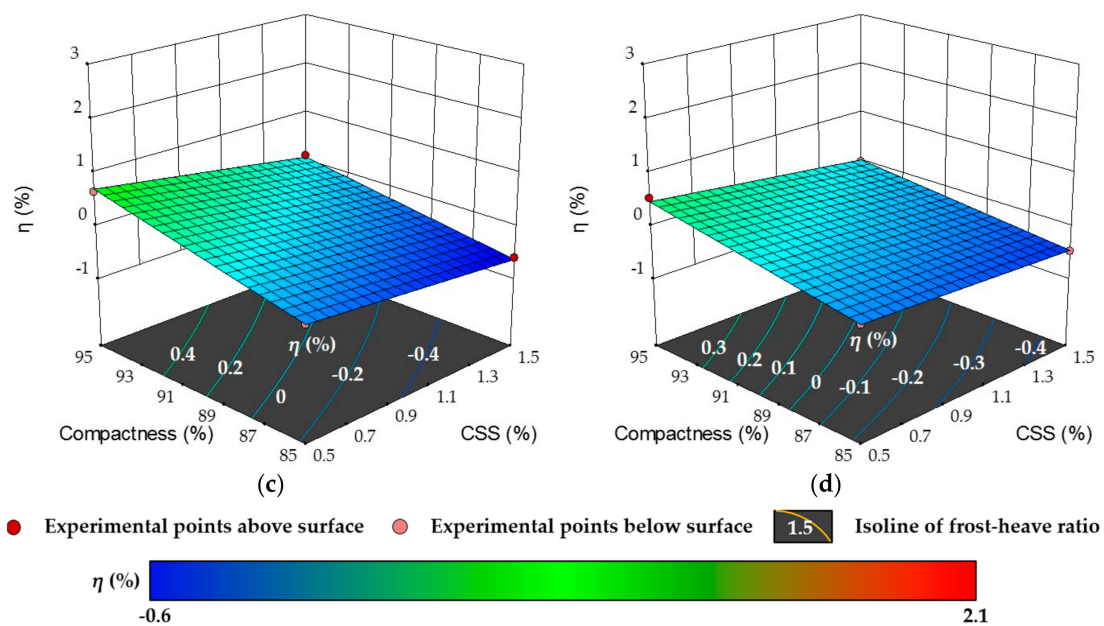


Figure 7. Three-dimensional surface plots of frost heave ratio response for compactness and CSS by (a) temperature -25 °C, water content 26%; (b) temperature -4 °C, water content 26%; (c) temperature -25 °C, water content 18%; and (d) temperature -4 °C, water content 18%.

For single factors, the results of the improved frost heave experiments indicated that the frost heave ratio was indeed a function of water content, compactness, and temperature, consistent with conclusions obtained from previous OFAT trials [35]. Sheng et al. [13] analyzed the sensitivity of the frost heave ratio of clay to compactness, temperature, and groundwater level, showing that this increased significantly as groundwater level increased, causing the water content of clay to increase and providing source material for ice lens formation and aggravated frost heave [36,37]. This demonstrates the positive correlation between water content and frost heave ratio. Similarly, the effect of temperature on frost heave in this study was consistent with past research [9,13,17].

Compactness was positively correlated with frost heave in this study. Uncompacted soil has high pore space that frozen ice lens cannot fill, while compacted soil has tightly structured soil particles with low pore space that is more easily filled by frozen ice lenses, leading to obvious frost heaving deformation [38]. This result was consistent with Sun et al. [21] and Bao [22], but other studies have concluded that increasing compactness reduces frost heave [13,39,40]. This contrast shows that the relationship between compactness and frost heave is affected by interactions [23] between compactness and other factors such as water content, as demonstrated in our analysis. The interaction factors $CSS \times WC$ and $C \times WC$ showed that these dynamics represent the failure of one factor to produce the same effect on the response at different levels of another factor [23]. When optimizing responses (minimize/maximum η) during engineering design and construction, it is necessary to consider such interactions. For example, in soil-filling projects (such as roadbeds, embankments, or dams), using low-CSS soil or mixed soil (adding coal ash or other materials) to fill the foundation, laying an anti-seepage layer to block moisture exchange, and increasing compactness all help to reduce the risk of frost heave [41–43].

3.2. Frost Heave Experiments

Soil parameter statistics and experimental results are compared in Table 6; 810 experiments were conducted by Bao [22] and complete data are given in Appendix A (Table A1). In order to consider the influence of interaction factors on η , $CSS \times WC$ and $C \times WC$ were added to the experimental data; the results of correlation analysis using SPSS 22.0 software are shown in Table 7.

Table 6. Statistical values of soil parameters and experimental results [22].

Statistical Values	Granulometric Composition			Water Content (%)	CSS (%)	Density (g/cm ³)	η (%)
	Clay (%)	Silt (%)	Sand (%)				
Maximum	53.46	49.89	8.18	24.80	0.92	1.90	3.50
Minimum	41.93	41.43	4.26	7.30	0.34	1.80	-0.60
Mean	48.91	45.58	5.50	17.18	0.53	1.87	0.74

Table 7. Correlation coefficients between η and various factors.

Response	Factor	Correlation Coefficient		
		Pearson	Kendall	Spearman
η	CSS	0.089*	0.042	0.048
	Compactness	0.338**	0.293**	0.373**
	Temperature	-0.289**	-0.255**	-0.351**
	Water content	0.628**	0.482**	0.614**
	C \times WC	0.701**	0.577**	0.720**
	CSS \times WC	0.234**	0.171**	0.232**

** : Correlation is significant at the 0.01 level. * : Correlation is significant at the 0.05 level.

The three correlation tests had consistent conclusions. The absolute value of the correlation coefficient between C \times WC and η was largest (significant at the 0.01 level). CSS \times WC was also significantly related to η at the 0.01 level. Of the four single factors, water content had the largest absolute coefficient value (positive), indicating that water content had a significant positive correlation relationship with η . Compactness was also significantly positively correlated with η , while temperature was negatively correlated. The Pearson test showed that the correlation between CSS and η was weakly positive at the 0.05 level, but the Kendall and Spearman test showed that the correlation between CSS and η was not significant. These results were consistent with the 16 improved frost heave experiments in showing that CSS had no significant effect on the frost heave ratio, while the others increased in effect from T < C < WC; the interaction factors CSS \times WC and C \times WC both had significant effects.

We used experimental data (Table A1) for correlation analysis to determine the relationship between frost heave ratio and different factors (consistent with Bao [22]) and the influence degree of factors on frost heave by correlation coefficient. After the interaction factors were added to the experimental data, the subsequent correlation analysis showed that the interaction factors did have a significant effect on frost heave, supporting our initial results. The conclusions from our 16 improved frost heave experiments were similar to those of the 810 OFAT frost heave experiments from Bao [22]: workload was reduced by 98.02%, demonstrating that the split-plot experimental design was helpful for obtaining reasonable results with reduced cost and workload. More importantly, interaction factors were more properly taken into account in the split-plot frost heave experimental design.

3.3. Prediction of Frost Heave Behavior

Table 8 shows the statistical indexes of the GRNN models. Figure 8 shows the results of the GRNN models' training and testing.

Table 8. Statistical indexes of generalized regression neural network (GRNN) models.

Statistical Indexes	Single-GRNN		Interact-GRNN	
	Training	Testing	Training	Testing
R ²	0.95	0.92	0.99	0.97
RMSE	0.2000	0.2370	0.1059	0.1373

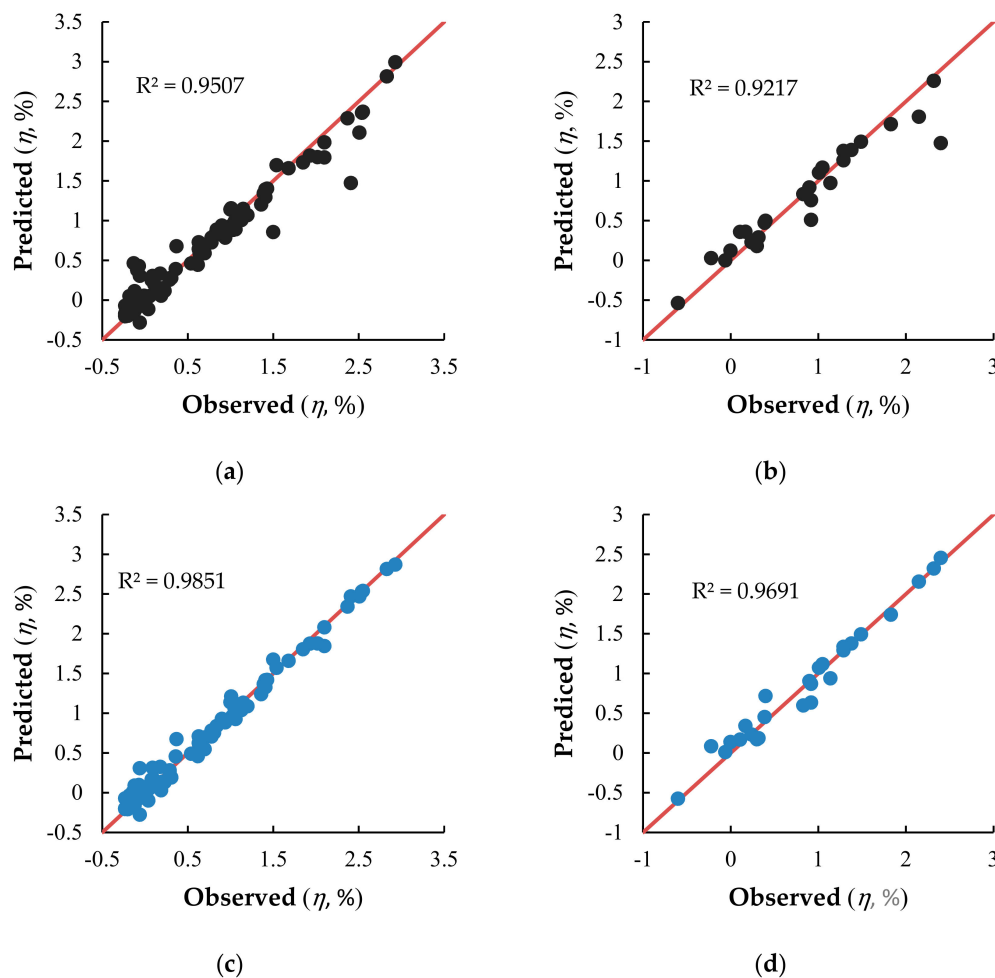


Figure 8. Relationship between observed and predicted η for the GRNN models: (a) training Single-GRNN, (b) testing Single-GRNN, (c) training Interact-GRNN, and (d) testing Interact-GRNN.

The training and testing R^2 values of the two GRNN models were all close to 1, indicating that the predicted values were very close to the experimental observations and demonstrating that the GRNN method can accurately predict frost heave behavior in the saline soil from the study area. Although the predicted values for Single-GRNN deviated from the 1:1 line, those for Interact-GRNN were all near this line, suggesting that the latter's prediction accuracy was higher. Table 8 supports this conclusion, as the training and testing R^2 values for Single-GRNN were 0.95 and 0.92, respectively, compared to those for Interact-GRNN (0.99 and 0.97, respectively), an increase of 3.62% and 5.14%, respectively. Similarly, the Single-GRNN training and testing RMSE values were 0.2000 and 0.2370, compared to those for Interact-GRNN (0.1059 and 0.1373, respectively), a decrease of 47.02% and 42.08%, respectively. Thus, we conclude that including interaction factors to the input dataset can significantly improve the GRNN results when simulated frost heave behavior of saline soil by reducing the deviation between predicted and observed values. In comparison, Zhang et al. [20] used BPNN and GRNN to obtain the frost heave ratio from data for water content, compactness, temperature, and content of soluble salt. Those results demonstrated that both methods were suitable for predicting the frost heave ratio of saline soil although the GRNN model was more accurate. However, that study did not include interaction factors in the input dataset for either model to improve the outputs. The testing R^2 (RMSE) value of GRNN in Zhang et al. [20] is 0.87 (0.2598), which is smaller (bigger) than R^2 0.97 (RMSE, 0.1373) of Interact-GRNN.

4. Conclusions

In order to determine interaction factors affecting frost heave and establish a high-accuracy GRNN model to predict the frost heave behavior of saline soil, split-plot frost heave experiments were conducted and a GRNN model including interaction factors was applied, with the following conclusions:

Of the single factors, water content had the greatest influence on the frost heave ratio (η) of unsaturated soil with a significant positively correlation. Factor compactness was also significantly positively correlated with η , while temperature was negatively correlated with η and CSS had no significant correlation. While these results are applicable to the study area's sodic saline soil and are consistent with other research [21,22], some studies on frost heave have shown that compactness is negatively correlated with frost heave. This is because the interactions between compactness and water content affect the relationship between compactness and frost heave. The split-plot experiment was able to analyze the influence degree of all single factors while considering the relationships between interaction factors and the response value. This study design can also be used in other multifactorial experiments including interaction factors and significantly reduces the experimental workload while optimizing the experimental arrangements. We only set two levels (low and high) for each factor and used a linear model to represent the relationship between frost heave and the influencing factors, but future research could set more factor levels and use a nonlinear model. Our results showed that interaction factors CSS \times WC and C \times WC had significant effects on the frost heave behavior of saline soil, as supported by correlation analysis. At low CSS (high compactness), the sensitivity of η was smaller than at high CSS (low compactness). This could be important for engineering design and construction in cold regions: for example, foundations could be covered with low-CSS soil to increase compactness and control frost heave damage. The accuracy of our results demonstrated that the GRNN model was suitable for predicting frost heave ratios in unsaturated saline soil in the study area, and that its performance was improved by the inclusion of interaction factors rather than single factors only.

Author Contributions: Conceptualization, H.W. and J.B.; Data curation, H.W.; Formal analysis, H.W.; Funding acquisition, J.B. and Y.W.; Methodology, H.W. and J.W.; Project administration, H.W. and X.S.; Resources, X.S.; Validation, H.W. and J.W.; Visualization, H.W. and Z.J.; Writing—original draft, H.W.; Writing—review & editing, H.W. and Y.W.

Funding: This research was funded by the National Key R&D Program of China, grant number 2018YFC1800400; the National Natural Science Foundation of China, grant number 41072255; the 111 Project, grant number B16020; and the National Natural Science Youth Fund, grant number 41807155.

Acknowledgments: The authors wish to thank Shuochao Bao for providing complete data of single-factor frost-heaving experiment.

Conflicts of Interest: The authors declare no conflict of interest. The funders had no role in the design of the study; in the collection, analyses, or interpretation of data; in the writing of the manuscript, or in the decision to publish the results.

Appendix A

Table A1. All data of frost-heaving experiments.

NO.	CSS (%)	Compactness (%)	Temperature (°C)	Water Content (%)	η (%)
1	1.5	95	−2	22	−0.09
2	1.5	95	−4	22	0.93
3	1.5	95	−25	26	2.00
4	1.5	95	−15	21	1.18
5	1.5	95	−15	20	0.72
6	1.5	95	0	24	−0.18
7	1.5	95	−20	21	1.23
8	1.5	95	−25	20	0.79
9	1.5	95	−6	26	1.64
10	1.5	95	−8	18	0.02

Table A1. Cont.

NO.	CSS (%)	Compactness (%)	Temperature (°C)	Water Content (%)	η (%)
11	1.5	95	-20	18	0.07
12	1.5	95	-10	18	0.01
13	1.5	95	-25	18	0.11
14	1.5	95	-8	24	1.61
15	1.5	95	-15	18	0.03
16	1.5	95	-8	22	1.25
17	1.5	95	-25	24	1.85
18	1.5	95	0	22	-0.07
19	1.5	95	-25	22	1.5
20	1.5	95	-8	20	0.67
21	1.5	95	-20	26	2.06
22	1.5	95	-15	22	1.41
23	1.5	95	0	26	-0.1
24	1.5	95	-10	20	0.67
25	1.5	95	-10	24	1.65
26	1.5	95	-15	26	2
27	1.5	95	-6	22	1.14
28	1.5	95	-6	24	1.43
29	1.5	95	-8	21	1.1
30	1.5	95	-2	18	-0.08
31	1.5	95	-4	24	1.23
32	1.5	95	-4	21	0.95
33	1.5	95	-2	24	-0.2
34	1.5	95	-10	21	1.11
35	1.5	95	-4	26	1.36
36	1.5	95	-2	26	-0.11
37	1.5	95	-25	21	1.27
38	1.5	95	-4	20	0.6
39	1.5	95	-2	21	-0.08
40	1.5	95	-6	18	0.02
41	1.5	95	0	20	-0.08
42	1.5	95	-15	24	1.76
43	1.5	95	-6	21	1.06
44	1.5	95	0	21	-0.07
45	1.5	95	-10	22	1.3
46	1.5	95	-20	22	1.44
47	1.5	95	0	18	-0.06
48	1.5	95	-20	20	0.76
49	0	85	-6	18	-0.01
50	0	85	-15	20	-0.06
51	0	85	-10	22	0.29
52	0	85	-8	21	0.25
53	0	85	-10	26	0.7
54	0	85	-15	21	0.25
55	0	85	-15	24	0.79
56	0	85	0	18	-0.01
57	0	85	-20	20	-0.07
58	0	85	-4	24	0.82
59	0	85	-20	24	0.81
60	0	85	-4	20	0
61	0	85	-4	18	-0.01
62	0	85	-4	26	0.68
63	0	85	-20	22	0.3

Table A1. Cont.

NO.	CSS (%)	Compactness (%)	Temperature (°C)	Water Content (%)	η (%)
64	0	85	-8	26	0.69
65	0	85	-6	21	0.25
66	0	85	-10	21	0.25
67	0	85	-10	24	0.78
68	0	85	-6	24	0.8
69	0	85	-25	20	-0.08
70	0	85	-6	20	-0.02
71	0	85	-2	22	0.3
72	0	85	-20	26	0.76
73	0	85	-15	18	-0.01
74	0	85	-10	20	-0.04
75	0	85	-25	22	0.3
76	0	85	-15	22	0.29
77	0	85	-6	22	0.29
78	0	85	-20	21	0.25
79	0	85	-25	26	0.78
80	0	85	-2	26	0.64
81	0	85	-8	18	-0.01
82	0	85	0	26	-0.07
83	0	85	-25	24	0.83
84	0	85	-8	24	0.78
85	0	85	0	21	0
86	0	85	-2	21	0.25
87	0	85	-8	22	0.29
88	0	85	-25	18	-0.01
89	0	85	-8	20	-0.03
90	0	85	0	24	-0.05
91	0	85	-25	21	0.25
92	0	85	0	20	0
93	0	85	-10	18	-0.01
94	0	85	-2	18	-0.01
95	0	85	-2	24	0.83
96	0.3	95	-10	21	1.23
97	0.3	95	-25	24	1.37
98	0.3	95	-6	18	0.7
99	0.3	95	-15	24	1.33
100	0.3	95	0	18	-0.05
101	0.3	95	-10	26	1.35
102	0.3	95	-10	24	1.29
103	0.3	95	-20	21	1.21
104	0.3	95	-20	20	1.13
105	0.3	95	-25	22	1.23
106	0.3	95	-20	24	1.35
107	0.3	95	-4	26	1.37
108	0.3	95	-2	18	0.68
109	0.3	95	-2	26	1.06
110	0.3	95	-10	18	0.75
111	0.3	95	-20	26	1.37
112	0.3	95	-15	20	1.13
113	0.3	95	-20	18	0.78
114	0.3	95	-2	22	1.14
115	0.3	95	0	26	-0.09
116	0.3	95	-2	21	1.06
117	0.3	95	-10	22	1.18
118	0.3	95	-10	20	1.13
119	0.3	95	-4	21	1.27

Table A1. Cont.

NO.	CSS (%)	Compactness (%)	Temperature (°C)	Water Content (%)	η (%)
120	0.3	95	-15	18	0.75
121	0.3	95	-25	26	1.39
122	0.3	95	-20	22	1.22
123	0.3	95	-15	21	1.22
124	0.3	95	-6	22	1.19
125	0.3	95	-4	20	1.2
126	0.3	95	-25	20	1.13
127	0.3	95	0	21	-0.03
128	0.3	95	-8	24	1.27
129	0.3	95	-4	22	1.2
130	0.3	95	0	22	-0.1
131	0.3	95	-8	18	0.72
132	0.3	95	-8	21	1.24
133	0.3	95	-8	20	1.15
134	0.3	95	0	20	-0.07
135	0.3	95	-6	24	1.26
136	0.3	95	-15	26	1.36
137	0.3	95	-6	26	1.36
138	0.3	95	-4	18	0.69
139	0.3	95	-6	21	1.25
140	0.3	85	-6	21	0.15
141	0.3	85	-6	22	0.25
142	0.3	85	-10	22	0.23
143	0.3	85	0	20	0
144	0.3	85	-2	24	0.92
145	0.3	85	-6	20	-0.06
146	0.3	85	-4	22	0.27
147	0.3	85	-15	26	1.23
148	0.3	85	-8	26	1.18
149	0.3	85	-20	20	-0.13
150	0.3	85	-4	21	0.15
151	0.3	85	-6	26	1.16
152	0.3	85	0	26	-0.03
153	0.3	85	-8	21	0.15
154	0.3	85	-25	20	-0.14
155	0.3	85	-15	22	0.23
156	0.3	85	-25	24	0.92
157	0.3	85	-4	24	0.92
158	0.3	85	-8	22	0.24
159	0.3	85	-15	20	-0.12
160	0.3	85	-8	18	-0.09
161	0.3	85	-15	24	0.9
162	0.3	85	-2	21	0.14
163	0.3	85	0	18	0
164	0.3	85	-10	21	0.15
165	0.3	85	-6	24	0.91
166	0.3	85	-25	18	-0.2
167	0.3	85	-4	18	-0.08
168	0.3	85	-10	18	-0.12
169	0.3	85	-10	24	0.89
170	0.3	85	-8	20	-0.09
171	0.3	85	-10	26	1.19
172	0.3	85	-8	24	0.9
173	0.3	85	-25	22	0.24
174	0.3	85	-25	26	1.27

Table A1. Cont.

NO.	CSS (%)	Compactness (%)	Temperature (°C)	Water Content (%)	η (%)
175	0.3	85	-4	20	-0.05
176	0.3	85	-25	21	0.16
177	0.3	85	-20	26	1.26
178	0.3	85	-6	18	-0.09
179	0.3	85	0	21	-0.03
180	0.3	85	-15	18	-0.18
181	0.3	85	-2	22	0.28
182	0.3	85	-20	22	0.23
183	0.3	85	0	24	-0.08
184	0.3	85	-20	18	-0.2
185	0.5	95	-15	24	1.4
186	0.5	95	-25	18	0.63
187	0.5	95	-10	20	1
188	0.5	95	0	18	-0.06
189	0.5	95	0	20	-0.04
190	0.5	95	-6	26	1.41
191	0.5	95	-8	18	0.56
192	0.5	95	-10	18	0.58
193	0.5	95	-6	20	1.01
194	0.5	95	-6	24	1.35
195	0.5	95	-2	21	1.05
196	0.5	95	0	24	-0.05
197	0.5	95	-2	18	0.29
198	0.5	95	-2	26	1.23
199	0.5	95	-4	22	1.36
200	0.5	95	-20	21	1.23
201	0.5	95	-15	18	0.63
202	0.5	95	-4	18	0.60
203	0.5	95	-4	21	1.14
204	0.5	95	-25	21	1.25
205	0.5	95	0	22	-0.01
206	0.5	95	-15	22	1.35
207	0.5	95	-25	20	1.02
208	0.5	95	-15	21	1.21
209	0.5	95	-25	24	1.43
210	0.5	95	-2	20	0.95
211	0.5	95	-4	24	1.38
212	0.5	95	-2	24	1.24
213	0.5	95	-8	21	1.16
214	0.5	95	-4	20	1.02
215	0.5	95	-4	26	1.37
216	0.5	95	-25	26	1.49
217	0.5	95	-2	22	0.52
218	0.5	95	-20	20	1.02
219	0.5	95	-6	21	1.15
220	0.5	95	-10	24	1.39
221	0.5	95	-8	20	1.01
222	0.5	95	0	21	-0.05
223	0.5	95	-15	26	1.48
224	0.5	95	-10	22	1.35
225	0.5	95	-20	18	0.66
226	0.5	95	-25	22	1.38
227	0.5	95	-20	24	1.41
228	0.5	95	-10	26	1.44

Table A1. Cont.

NO.	CSS (%)	Compactness (%)	Temperature (°C)	Water Content (%)	η (%)
229	0.5	95	-20	22	1.38
230	1.2	90	-25	26	3.11
231	1.2	90	-20	26	2.97
232	1.2	90	-8	24	1.38
233	1.2	90	-15	20	0.36
234	1.2	90	0	21	-0.041
235	1.2	90	-15	18	0
236	1.2	90	-10	24	1.4
237	1.2	90	-2	20	0.08
238	1.2	90	-15	24	1.46
239	1.2	90	-8	26	2.83
240	1.2	90	-4	18	0
241	1.2	90	-10	26	2.86
242	1.2	90	-2	18	0
243	1.2	90	-4	22	0.61
244	1.2	90	-10	18	0
245	1.2	90	-25	22	0.71
246	1.2	90	-10	21	0.64
247	1.2	90	-4	21	0.61
248	1.2	90	-6	24	1.36
249	1.2	90	-6	21	0.62
250	1.2	90	-20	24	1.5
251	1.2	90	0	18	0
252	1.2	90	-2	21	-0.01
253	1.2	90	-4	24	1.33
254	1.2	90	-4	26	2.71
255	1.2	90	-25	21	0.7
256	1.2	90	-6	26	2.79
257	1.2	90	-25	18	0
258	1.2	90	-8	21	0.63
259	1.2	90	-25	20	0.37
260	1.2	90	0	20	-0.04
261	1.2	90	-2	22	0.22
262	1.2	90	-2	26	0.76
263	1.2	90	-6	22	0.62
264	1.2	90	-2	24	1.23
265	1.2	90	-20	18	0
266	1.2	90	0	22	-0.04
267	1.2	90	-20	22	0.71
268	1.2	90	-4	20	0.48
269	1.2	90	-10	20	0.39
270	1.2	90	-15	22	0.7
271	1.2	90	-8	20	0.39
272	1.5	85	-4	20	0.4
273	1.5	85	-2	20	-0.08
274	1.5	85	-6	24	1.03
275	1.5	85	-20	21	0.54
276	1.5	85	-4	22	0.75
277	1.5	85	-10	20	0.34
278	1.5	85	-8	22	0.85
279	1.5	85	0	22	-0.11
280	1.5	85	0	26	-0.07
281	1.5	85	0	21	-0.12
282	1.5	85	-10	24	1.16
283	1.5	85	-15	26	1.86
284	1.5	85	-15	24	1.25

Table A1. Cont.

NO.	CSS (%)	Compactness (%)	Temperature (°C)	Water Content (%)	η (%)
285	1.5	85	-10	21	0.38
286	1.5	85	-2	24	0.25
287	1.5	85	-2	21	-0.14
288	1.5	85	-2	18	-0.06
289	1.5	85	-25	22	1.08
290	1.5	85	-4	24	0.89
291	1.5	85	-25	18	-0.55
292	1.5	85	-6	21	0.23
293	1.5	85	-4	26	1.80
294	1.5	85	-15	21	0.48
295	1.5	85	-6	22	0.82
296	1.5	85	0	18	-0.05
297	1.5	85	0	20	-0.07
298	1.5	85	-8	20	0.35
299	1.5	85	-10	18	-0.58
300	1.5	85	-6	26	1.8
301	1.5	85	0	24	0.22
302	1.5	85	-4	21	0.09
303	1.5	85	-20	26	1.9
304	1.5	85	-8	26	1.8
305	1.5	85	-8	24	1.12
306	1.5	85	-15	20	0.36
307	1.5	85	-6	18	-0.53
308	1.5	85	-2	22	-0.12
309	1.5	85	-20	24	1.3
310	1.5	85	-20	18	-0.6
311	1.5	85	-10	26	1.8
312	1.5	85	-15	18	-0.6
313	1.5	85	-6	20	0.37
314	1.5	85	-25	21	0.57
315	1.5	85	-20	20	0.38
316	1.5	85	-4	18	-0.42
317	1.5	85	-8	18	-0.57
318	0.5	85	-10	21	0.19
319	0.5	85	-2	18	-0.06
320	0.5	85	-6	24	0.99
321	0.5	85	-15	20	-0.22
322	0.5	85	-10	26	1.29
323	0.5	85	-15	21	0.18
324	0.5	85	-2	20	-0.16
325	0.5	85	-8	22	0.25
326	0.5	85	-4	21	0.23
327	0.5	85	-6	22	0.26
328	0.5	85	-20	21	0.18
329	0.5	85	-25	24	0.99
330	0.5	85	-20	24	0.99
331	0.5	85	-20	26	1.41
332	0.5	85	-10	18	-0.23
333	0.5	85	-2	22	0.21
334	0.5	85	-2	24	0.58
335	0.5	85	-4	24	0.99
336	0.5	85	-6	18	-0.23
337	0.5	85	-6	26	1.29
338	0.5	85	0	21	-0.03

Table A1. Cont.

NO.	CSS (%)	Compactness (%)	Temperature (°C)	Water Content (%)	η (%)
339	0.5	85	-20	22	0.23
340	0.5	85	-20	20	-0.22
341	0.5	85	-4	18	-0.30
342	0.5	85	-15	26	1.34
343	0.5	85	0	26	-0.03
344	0.5	85	-10	24	0.97
345	0.5	85	-6	20	-0.19
346	0.5	85	-25	20	-0.22
347	0.5	85	0	22	-0.02
348	0.5	85	-8	26	1.3
349	0.5	85	-25	26	1.46
350	0.5	85	0	20	-0.01
351	0.5	85	-2	21	0.22
352	0.5	85	-8	24	0.99
353	0.5	85	-15	18	-0.23
354	0.5	85	-25	22	0.23
355	0.5	85	-25	18	-0.22
356	0.5	85	-8	20	-0.21
357	0.5	85	0	18	0
358	0.5	85	-8	21	0.19
359	0.5	85	-6	21	0.19
360	0.5	85	-25	21	0.19
361	0.5	85	-10	20	-0.22
362	0.5	90	-15	18	0.06
363	0.5	90	-20	22	0.94
364	0.5	90	-2	26	1.3
365	0.5	90	-15	21	0.92
366	0.5	90	-4	21	0.83
367	0.5	90	-10	24	1
368	0.5	90	-2	20	0.42
369	0.5	90	-6	20	0.33
370	0.5	90	-8	26	1.37
371	0.5	90	0	22	-0.02
372	0.5	90	-8	21	0.85
373	0.5	90	-15	26	1.41
374	0.5	90	0	26	-0.06
375	0.5	90	-8	24	0.98
376	0.5	90	-20	18	0.05
377	0.5	90	-20	20	0.4
378	0.5	90	-10	26	1.39
379	0.5	90	-2	18	-0.02
380	0.5	90	-6	26	1.37
381	0.5	90	-10	18	0.08
382	0.5	90	-8	22	0.93
383	0.5	90	-4	22	0.96
384	0.5	90	-15	20	0.36
385	0.5	90	0	18	-0.01
386	0.5	90	-8	18	0.1
387	0.5	90	-8	20	0.35
388	0.5	90	-6	18	0.1
389	0.5	90	-25	21	0.95
390	0.5	90	-4	20	0.32
391	0.5	90	-6	22	0.94
392	0.5	90	0	24	-0.06
393	0.5	90	-2	24	0.85
394	0.5	90	-4	18	0.11

Table A1. Cont.

NO.	CSS (%)	Compactness (%)	Temperature (°C)	Water Content (%)	η (%)
395	0.5	90	0	21	-0.06
396	0.5	90	-6	21	0.84
397	0.5	90	-10	21	0.9
398	0.5	90	-6	24	0.96
399	0.5	90	-25	18	0.04
400	0.5	90	-2	22	0.97
401	0.5	90	-10	22	0.92
402	0.5	90	-25	22	0.95
403	0.5	90	-25	24	1.19
404	0.5	90	-25	20	0.4
405	0.5	90	-25	26	1.45
406	0.5	90	-20	26	1.43
407	0	95	-15	22	2.09
408	0	95	-8	26	2.05
409	0	95	-2	18	1.14
410	0	95	-20	18	1.05
411	0	95	-4	22	2.07
412	0	95	-8	21	2.07
413	0	95	0	21	-0.03
414	0	95	-10	20	1.57
415	0	95	-25	22	2.12
416	0	95	-2	24	2.49
417	0	95	-10	21	2.06
418	0	95	-6	21	2.07
419	0	95	-6	18	1.12
420	0	95	-10	18	1.1
421	0	95	-10	26	2.06
422	0	95	-25	20	1.56
423	0	95	-15	26	2.11
424	0	95	-4	20	1.64
425	0	95	-8	20	1.59
426	0	95	-10	24	2.52
427	0	95	-25	21	2.1
428	0	95	-15	24	2.51
429	0	95	-20	21	2.08
430	0	95	-10	22	2.08
431	0	95	-20	20	1.56
432	0	95	-2	26	1.94
433	0	95	-20	24	2.52
434	0	95	-15	18	1.05
435	0	95	-15	21	2.07
436	0	95	0	24	-0.04
437	0	95	-8	18	1.11
438	0	95	-6	26	2.03
439	0	95	0	20	-0.04
440	0	95	-4	21	2.08
441	0	95	-6	20	1.65
442	0	95	-4	18	1.11
443	0	95	-25	26	2.15
444	0	95	-6	24	2.51
445	0	95	-25	18	1.05
446	0	95	-2	21	1.95
447	0	95	-8	24	2.51
448	0	95	0	26	-0.05
449	0	95	-15	20	1.56
450	0	95	0	22	-0.03

Table A1. Cont.

NO.	CSS (%)	Compactness (%)	Temperature (°C)	Water Content (%)	η (%)
451	1.2	85	0	26	-0.07
452	1.2	85	-2	26	0.26
453	1.2	85	-4	22	0.24
454	1.2	85	-8	24	0.98
455	1.2	85	-6	18	-0.48
456	1.2	85	-4	26	1.46
457	1.2	85	-10	20	-0.14
458	1.2	85	-15	18	-0.54
459	1.2	85	-10	26	1.68
460	1.2	85	-15	20	-0.17
461	1.2	85	-25	20	-0.18
462	1.2	85	-10	24	1
463	1.2	85	-20	18	-0.55
464	1.2	85	-4	20	-0.09
465	1.2	85	0	20	-0.04
466	1.2	85	-2	18	-0.35
467	1.2	85	-15	22	0.31
468	1.2	85	-8	21	0.19
469	1.2	85	-10	18	-0.52
470	1.2	85	-10	21	0.17
471	1.2	85	-6	22	0.26
472	1.2	85	-25	18	-0.56
473	1.2	85	-4	21	0.23
474	1.2	85	-2	20	-0.03
475	1.2	85	-6	24	0.96
476	1.2	85	0	18	0
477	1.2	85	-20	26	1.77
478	1.2	85	-2	21	0.15
479	1.2	85	-15	26	1.74
480	1.2	85	-15	24	1.03
481	1.2	85	0	21	-0.01
482	1.2	85	-25	21	0.17
483	1.2	85	-8	26	1.67
484	1.2	85	-8	18	-0.5
485	1.2	85	-4	18	-0.43
486	1.2	85	-10	22	0.28
487	1.2	85	-25	22	0.32
488	1.2	85	-8	20	-0.13
489	1.2	85	-2	24	0.85
490	1.2	85	-20	22	0.32
491	1.2	85	-8	22	0.27
492	1.2	85	-6	26	1.57
493	1.2	85	-2	22	-0.03
494	1.2	85	-6	21	0.2
495	1.2	85	0	24	-0.06
496	1.2	85	-6	20	-0.11
497	0.3	90	-6	22	0.49
498	0.3	90	-15	18	-0.12
499	0.3	90	-2	24	0.85
500	0.3	90	-6	24	0.82
501	0.3	90	-15	20	0.06
502	0.3	90	-25	18	-0.14
503	0.3	90	-2	18	-0.05
504	0.3	90	-25	22	0.46
505	0.3	90	-10	22	0.47

Table A1. Cont.

NO.	CSS (%)	Compactness (%)	Temperature (°C)	Water Content (%)	η (%)
506	0.3	90	-2	22	0.53
507	0.3	90	-4	20	0.11
508	0.3	90	-10	18	-0.11
509	0.3	90	-10	21	0.21
510	0.3	90	0	22	-0.07
511	0.3	90	-8	26	1.24
512	0.3	90	-8	24	0.81
513	0.3	90	-8	22	0.48
514	0.3	90	-15	22	0.47
515	0.3	90	-20	26	1.31
516	0.3	90	0	21	0
517	0.3	90	-20	22	0.46
518	0.3	90	-8	20	0.1
519	0.3	90	-6	18	-0.06
520	0.3	90	-25	20	0.04
521	0.3	90	-2	20	-0.02
522	0.3	90	-15	21	0.2
523	0.3	90	-4	26	1.2
524	0.3	90	-6	21	0.22
525	0.3	90	0	24	-0.09
526	0.3	90	-4	24	0.84
527	0.3	90	-20	21	0.2
528	0.3	90	-25	21	0.2
529	0.3	90	0	20	-0.01
530	0.3	90	-10	20	0.08
531	0.3	90	-10	26	1.26
532	0.3	90	-8	18	-0.09
533	0.3	90	-4	22	0.51
534	0.3	90	-20	24	0.84
535	0.3	90	-2	26	1.06
536	0.3	90	-15	26	1.29
537	0.3	90	-20	18	-0.13
538	0.3	90	0	26	-0.16
539	0.3	90	-4	21	0.24
540	0.3	90	-20	20	0.05
541	0.3	90	-4	18	-0.05
542	0.3	90	-8	21	0.21
543	0.3	90	0	18	0
544	0.3	90	-2	21	0.25
545	0.3	90	-10	24	0.81
546	0.3	90	-6	20	0.1
547	1.2	95	-2	21	-0.06
548	1.2	95	-10	22	1.42
549	1.2	95	-8	20	1.27
550	1.2	95	-2	22	1.09
551	1.2	95	-2	24	0.36
552	1.2	95	-20	20	1.41
553	1.2	95	-2	18	-0.11
554	1.2	95	-8	26	1.59
555	1.2	95	-20	24	1.55
556	1.2	95	-25	22	1.56
557	1.2	95	-4	24	1.5
558	1.2	95	-8	22	1.4
559	1.2	95	-25	18	0.57
560	1.2	95	-4	18	0.51
561	1.2	95	-20	22	1.51

Table A1. Cont.

NO.	CSS (%)	Compactness (%)	Temperature (°C)	Water Content (%)	η (%)
562	1.2	95	-15	24	1.52
563	1.2	95	-4	26	1.46
564	1.2	95	-15	21	1.41
565	1.2	95	-2	26	1.08
566	1.2	95	0	20	-0.07
567	1.2	95	0	24	-0.07
568	1.2	95	-20	26	1.77
569	1.2	95	-15	20	1.37
570	1.2	95	-6	26	1.54
571	1.2	95	-6	22	1.41
572	1.2	95	-8	24	1.49
573	1.2	95	0	22	-0.03
574	1.2	95	-6	24	1.5
575	1.2	95	-20	18	0.54
576	1.2	95	-4	20	1.16
577	1.2	95	-25	24	1.64
578	1.2	95	-10	20	1.3
579	1.2	95	-6	21	1.26
580	1.2	95	-6	18	0.54
581	1.2	95	-25	20	1.44
582	1.2	95	-4	21	1.23
583	1.2	95	-15	22	1.47
584	1.2	95	-4	22	1.36
585	1.2	95	-15	26	1.72
586	1.2	95	-10	18	0.54
587	1.5	90	-6	21	0.77
588	1.5	90	0	24	-0.14
589	1.5	90	-4	26	2.42
590	1.5	90	-2	20	-0.1
591	1.5	90	-25	20	0.79
592	1.5	90	-25	24	1.82
593	1.5	90	0	18	-0.06
594	1.5	90	-10	21	0.96
595	1.5	90	-2	18	-0.07
596	1.5	90	-2	22	-0.13
597	1.5	90	-4	18	-0.12
598	1.5	90	-20	26	3.46
599	1.5	90	0	20	-0.09
600	1.5	90	-25	18	-0.14
601	1.5	90	-6	24	1.47
602	1.5	90	-2	24	-0.22
603	1.5	90	-15	20	0.71
604	1.5	90	-15	18	-0.19
605	1.5	90	0	21	-0.1
606	1.5	90	-6	22	0.9
607	1.5	90	-4	20	0.58
608	1.5	90	-8	20	0.61
609	1.5	90	-8	18	-0.19
610	1.5	90	-20	21	1.05
611	1.5	90	-20	22	1.08
612	1.5	90	-20	18	-0.16
613	1.5	90	-15	26	3.37
614	1.5	90	-8	22	0.99
615	1.5	90	-8	26	3.19
616	1.5	90	-10	26	3.25

Table A1. Cont.

NO.	CSS (%)	Compactness (%)	Temperature (°C)	Water Content (%)	η (%)
617	1.5	90	-6	26	3
618	1.5	90	-4	22	0.76
619	1.5	90	-25	26	3.5
620	1.5	90	-10	22	1.02
621	1.5	90	-2	26	-0.16
622	1.5	90	-15	21	1.01
623	1.5	90	-20	20	0.75
624	1.5	90	-8	21	0.82
625	1.5	90	-25	22	1.12
626	1.5	90	-10	18	-0.22
627	1.5	90	-25	21	1.09
628	1.5	90	0	22	-0.12
629	1.5	90	-6	18	-0.17
630	1.5	90	-6	20	0.59
631	1.5	90	-10	24	1.65
632	1.5	90	-15	24	1.75
633	0	90	-2	22	0.6
634	0	90	-15	24	2.57
635	0	90	-15	21	0.62
636	0	90	-15	22	0.67
637	0	90	-2	24	2.5
638	0	90	-4	20	0.18
639	0	90	-6	24	2.55
640	0	90	-6	26	2.32
641	0	90	-6	22	0.68
642	0	90	-25	24	2.61
643	0	90	-15	18	0.02
644	0	90	-6	18	0.05
645	0	90	-10	24	2.54
646	0	90	-4	18	0.07
647	0	90	-25	22	0.67
648	0	90	-8	22	0.67
649	0	90	-20	26	2.4
650	0	90	-10	21	0.62
651	0	90	-8	24	2.54
652	0	90	-20	20	0.15
653	0	90	-20	18	0.02
654	0	90	-2	20	0.17
655	0	90	-15	20	0.15
656	0	90	0	21	0
657	0	90	-4	21	0.64
658	0	90	-20	24	2.59
659	0	90	-6	21	0.63
660	0	90	-2	21	0.58
661	0	90	-25	18	0.02
662	0	90	-8	18	0.03
663	0	90	-6	20	0.17
664	0	90	-25	26	2.41
665	0	90	-4	26	2.31
666	0	90	-25	20	0.24
667	0	90	0	20	-0.01
668	0	90	-15	26	2.37
669	0	90	-8	20	0.16
670	0	90	-8	21	0.63
671	0	90	-25	21	0.62
672	0	90	-20	22	0.67

Table A1. Cont.

NO.	CSS (%)	Compactness (%)	Temperature (°C)	Water Content (%)	η (%)
673	0	90	-20	21	0.62
674	0	90	-10	22	0.67
675	0	90	-4	24	2.56
676	0	90	0	26	-0.06
677	0	90	0	18	0
678	0	90	-2	26	2.22
679	0	90	-4	22	0.69
680	0	90	-10	18	0.03
681	1.5	95	-4	18	0.02
682	1.5	95	-10	26	1.89
683	1.5	95	-6	20	0.65
684	1.5	95	-8	26	1.83
685	1.5	95	-2	20	-0.1
686	1.5	95	-20	24	1.81
687	0	85	0	22	-0.02
688	0	85	-15	26	0.74
689	0	85	-20	18	-0.01
690	0	85	-6	26	0.68
691	0	85	-2	20	0.03
692	0	85	-4	21	0.25
693	0	85	-4	22	0.3
694	0.3	95	-2	20	1.2
695	0.3	95	-15	22	1.2
696	0.3	95	-6	20	1.17
697	0.3	95	-25	18	0.78
698	0.3	95	-2	24	1.01
699	0.3	95	-8	26	1.36
700	0.3	95	-8	22	1.18
701	0.3	95	-4	24	1.23
702	0.3	95	-25	21	1.21
703	0.3	95	0	24	-0.09
704	0.3	85	0	22	-0.02
705	0.3	85	-2	18	-0.03
706	0.3	85	-4	26	1.13
707	0.3	85	-2	20	-0.05
708	0.3	85	-2	26	1.03
709	0.3	85	-15	21	0.15
710	0.3	85	-20	21	0.16
711	0.3	85	-20	24	0.91
712	0.3	85	-10	20	-0.11
713	0.5	95	-20	26	1.5
714	0.5	95	-10	21	1.18
715	0.5	95	-8	26	1.43
716	0.5	95	0	26	-0.05
717	0.5	95	-8	24	1.39
718	0.5	95	-8	22	1.35
719	0.5	95	-15	20	1.01
720	0.5	95	-6	22	1.36
721	0.5	95	-6	18	0.54
722	1.2	90	-15	26	2.93
723	1.2	90	0	24	-0.06
724	1.2	90	0	26	-0.07
725	1.2	90	-10	22	0.63
726	1.2	90	-8	18	0
727	1.2	90	-25	24	1.54

Table A1. Cont.

NO.	CSS (%)	Compactness (%)	Temperature (°C)	Water Content (%)	η (%)
728	1.2	90	-20	20	0.36
729	1.2	90	-15	21	0.68
730	1.2	90	-8	22	0.62
731	1.2	90	-6	20	0.42
732	1.2	90	-20	21	0.7
733	1.2	90	-6	18	0
734	1.5	85	-25	20	0.4
735	1.5	85	-10	22	0.9
736	1.5	85	-25	24	1.34
737	1.5	85	-8	21	0.31
738	1.5	85	-20	22	1.05
739	1.5	85	-2	26	-0.08
740	1.5	85	-15	22	1
741	1.5	85	-25	26	1.93
742	0.5	85	0	24	-0.02
743	0.5	85	-8	18	-0.23
744	0.5	85	-15	22	0.23
745	0.5	85	-4	20	-0.18
746	0.5	85	-15	24	0.98
747	0.5	85	-4	22	0.27
748	0.5	85	-20	18	-0.23
749	0.5	85	-4	26	1.31
750	0.5	85	-10	22	0.24
751	0.5	85	-2	26	0.57
752	0.5	90	-20	21	0.94
753	0.5	90	-15	22	0.93
754	0.5	90	-4	26	1.37
755	0.5	90	-4	24	0.94
756	0.5	90	-15	24	1.03
757	0.5	90	-20	24	1.05
758	0.5	90	-10	20	0.39
759	0.5	90	-2	21	0.53
760	0.5	90	0	20	-0.03
761	0	95	-6	22	2.07
762	0	95	-2	22	1.98
763	0	95	-4	26	2.02
764	0	95	-20	26	2.13
765	0	95	-8	22	2.07
766	0	95	0	18	-0.02
767	0	95	-2	20	1.66
768	0	95	-4	24	2.5
769	0	95	-25	24	2.54
770	0	95	-20	22	2.1
771	1.2	85	0	22	-0.02
772	1.2	85	-25	26	1.81
773	1.2	85	-20	24	1.05
774	1.2	85	-4	24	0.94
775	1.2	85	-20	21	0.17
776	1.2	85	-15	21	0.17
777	1.2	85	-25	24	1.19
778	1.2	85	-20	20	-0.17
779	0.3	90	-6	26	1.23
780	0.3	90	-25	26	1.31
781	0.3	90	-25	24	0.84
782	0.3	90	-15	24	0.83
783	1.2	95	-20	21	1.43
784	1.2	95	-25	21	1.54

Table A1. Cont.

NO.	CSS (%)	Compactness (%)	Temperature (°C)	Water Content (%)	η (%)
785	1.2	95	−8	21	1.27
786	1.2	95	−15	18	0.54
787	1.2	95	−10	26	1.64
788	1.2	95	−8	18	0.54
789	1.2	95	−10	24	1.49
790	1.2	95	−2	20	−0.11
791	1.2	95	0	18	−0.07
792	1.2	95	−6	20	1.24
793	1.2	95	0	26	−0.03
794	1.2	95	−10	21	1.3
795	1.2	95	0	21	−0.04
796	1.2	95	−25	26	1.95
797	1.5	90	−4	21	0.64
798	1.5	90	0	26	−0.12
799	1.5	90	−15	22	1.07
800	1.5	90	−4	24	1.34
801	1.5	90	−20	24	1.8
802	1.5	90	−8	24	1.61
803	1.5	90	−10	20	0.63
804	1.5	90	−2	21	−0.11
805	0	90	−10	26	2.32
806	0	90	−2	18	0.09
807	0	90	0	22	−0.02
808	0	90	−10	20	0.16
809	0	90	0	24	−0.04
810	0	90	−8	26	2.32

References

- Zeng, G.; Zhang, M.; Li, Z.; Pei, W. Study of moisture migration and frost heave model of freezing saturated soil. *Rock Soil Mech.* **2015**, *1085–1092*. [[CrossRef](#)]
- Yin, X.; Liu, E.; Song, B.; Zhang, D. Numerical analysis of coupled liquid water, vapor, stress and heat transport in unsaturated freezing soil. *Cold Reg. Sci. Technol.* **2018**, *155*, 20–28. [[CrossRef](#)]
- She, W.; Cao, X.; Zhao, G.; Cai, D.; Jiang, J.; Hu, X. Experimental and numerical investigation of the effect of soil type and fineness on soil frost heave behavior. *Cold Reg. Sci. Technol.* **2018**, *148*, 148–158. [[CrossRef](#)]
- Bai, R.; Lai, Y.; Zhang, M.; Gao, J. Water-vapor-heat behavior in a freezing unsaturated coarse-grained soil with a closed top. *Cold Reg. Sci. Technol.* **2018**, *155*, 120–126. [[CrossRef](#)]
- Gao, J.; Lai, Y.; Zhang, M.; Feng, Z.; Gao, J.; Lai, Y.; Zhang, M.; Feng, Z.; Gao, J.; Lai, Y. Experimental study on the water-heat-vapor behavior in a freezing coarse-grained soil. *Appl. Therm. Eng.* **2018**, *128*, 956–965. [[CrossRef](#)]
- Kong, Y. Experimental Research on the Saline Soil Water-Salt Transport and Structure Evolution in Zhenlai Zone. Ph.D. Thesis, Jilin University, Jilin, China, 2017.
- Li, S.; Lai, Y.; Pei, W.; Zhang, S.; Zhong, H. Moisture–temperature changes and freeze–thaw hazards on a canal in seasonally frozen regions. *Nat. Hazards* **2014**, *72*, 287–308. [[CrossRef](#)]
- Yu, F.; Qi, J.; Zhang, M.; Lai, Y.; Yao, X.; Liu, Y.; Wu, G. Cooling performance of two-phase closed thermosyphons installed at a highway embankment in permafrost regions. *Appl. Therm. Eng.* **2016**, *98*, 220–227. [[CrossRef](#)]
- Tai, B.; Liu, J.; Li, X.; Yue, Z.; Shen, Y. Numerical model of frost heaving and anti-frost heave measures of high speed railway subgrade in cold region. *China Railw. Sci.* **2017**, 1–9. [[CrossRef](#)]
- Wang, T.; Yue, Z. Influence of fines content on frost heaving properties of coarse grained soil. *Rock Soil Mech.* **2013**, *34*, 359–364, 388. [[CrossRef](#)]
- Gilpin, R.R. A model for the prediction of ice lensing and frost heave in soils. *Water Resour. Res.* **1980**, *16*, 918–930. [[CrossRef](#)]

12. Sheng, D.; Axelsson, K.; Knutsson, S. Frost Heave due to Ice Lens Formation in Freezing Soils 1. Theory and Verification. *Nord. Hydrol.* **1995**, *26*, 125–146. [[CrossRef](#)]
13. Sheng, D.; Zhang, S.; He, Z. Assessing frost susceptibility of soils. *Chin. J. Rock Mech. Eng.* **2014**, 594–605. [[CrossRef](#)]
14. Zheng, H.; Kanie, S. The application of Mixed Hybrid FEM in the frost heave prediction verified by FEM and indoor frost heave experiments. *Cold Reg. Sci. Technol.* **2017**, *142*, 85–92. [[CrossRef](#)]
15. Singh, A.K.; Chaudhary, D.R. Evaluation of heat and moisture transfer properties in a frozen-unfrozen water-soil system. *Int. J. Heat Mass Transf.* **1995**, *38*, 2297–2303. [[CrossRef](#)]
16. Zhang, X.; Zhang, M.; Lu, J.; Pei, W.; Yan, Z. Effect of hydro-thermal behavior on the frost heave of a saturated silty clay under different applied pressures. *Appl. Therm. Eng.* **2017**, *117*, 462–467. [[CrossRef](#)]
17. Zhang, P.; Huang, X.; Yang, X.; Liu, Z.; Zhong, Z. Experiment on coupling effect of water and thermal field and salt-expansion deformation of salty soil. *Rock Soil Mech.* **2018**, 1–6. [[CrossRef](#)]
18. Wu, Q.; Zhu, Y. Experimental studies on salt expansion for coarse grain soil under constant temperature. *Cold Reg. Sci. Technol.* **2002**, *34*, 59–65. [[CrossRef](#)]
19. Wan, X.-S.; Liao, M.-K.; Du, L.-Q. Experimental Study on the Influence of Temperature on Salt Expansion of Sodium Sulfate Saline Soil. *J. Highw. Transp. Res. Dev. (Engl. Ed.)* **2017**, *11*. [[CrossRef](#)]
20. Zhang, X.; Wang, Q.; Huo, Z.; Yu, T.; Wang, G.; Liu, T.; Wang, W. Prediction of frost-heaving behavior of saline soil in western Jilin Province, China, by neural network methods. *Math. Probl. Eng.* **2017**, *2017*, 1–10. [[CrossRef](#)]
21. Sun, D.; Wang, W.; Wang, Q.; Chen, J.; Niu, C.; Cao, C. Characteristics and prediction of frost heave of saline soil in western Jilin Province. *Int. J. Heat Technol.* **2016**, *34*, 709–714. [[CrossRef](#)]
22. Bao, S.C. Frost Heaving Characteristic and PFC-3D Numerical Analysis of Saline Soil in Western Jilin Province. Ph.D. Thesis, Jilin University, Jilin, China, 2015.
23. Montgomery, D. Design and Analysis of Experiments, 8th ed. 111 River Street; John Wiley & Sons, Inc.: Hoboken, NJ, USA, 2012.
24. He, Z.; Liang, Z. Experimental Design for Split-plot with Related Factors. *Syst. Eng. Theory Pract.* **2009**, *29*, 56–63. [[CrossRef](#)]
25. Jones, B.; Nachtsheim, C.J. Split-Plot Designs: What, Why, and How. *J. Qual. Technol.* **2009**, *41*, 361. [[CrossRef](#)]
26. Bingham, D.; Sitter, R.R. Fractional factorial split-plot designs for robust parameter experiments. *Technometrics* **2003**, *45*, 80–89. [[CrossRef](#)]
27. Celikoglu, H.B. A Dynamic Network Loading Model for Traffic Dynamics Modeling. *IEEE Trans. Intell. Transp. Syst.* **2007**, *8*, 575–583. [[CrossRef](#)]
28. Yu, T. Numerical Analysis of Coupled Water Heat Salt and Stress of Saline Soil in Western Jilin Province. Ph.D. Thesis, Jilin University, Jilin, China, 2016.
29. Zhang, D.; Wang, S. Mechanism of freeze-thaw action in land salinization process—As an sample in west Jilin Province. *Bull. Soil Water Conserv.* **2000**, *20*, 14–17. [[CrossRef](#)]
30. Bao, S.D. *Soil Agro-chemical Analysis*, 3rd ed.; China Agriculture Press: Beijing, China, 2008.
31. StatEase. Design-Export. Available online: <https://www.statease.com/> (accessed on 31 July 2019).
32. Kenward, M.G.; Roger, J. Small sample inference for fixed effects from restricted maximum likelihood. *Biometrics* **1997**, *53*, 983–997. [[CrossRef](#)]
33. Box, G.; Jones, S. Split-plot designs for robust product experimentation. *J. Appl. Stat.* **1992**, *19*, 3–26. [[CrossRef](#)]
34. Specht, D.F. A general regression neural network. *IEEE Trans. Neural Netw.* **1991**, *2*, 568–576. [[CrossRef](#)]
35. Chen, X.; Lu, G.; Zhu, J. Research on improvement of indoor frost-heave ratio experiment method. *J. Northwest. Univ. (Nat. Sci. Ed.)* **2010**, *40*, 145–149.
36. Ma, W.; Wang, D. Studies on frozen soil mechanics in China in past 50 years and their prospect. *Chin. J. Geotech. Eng.* **2012**, *34*, 625–640.
37. Zhou, G. Analysis of mechanism of rest raining soil freezing swelling by using intermission method. *Coll. Civ. Archit. Eng.* **1999**, *28*, 413–416. [[CrossRef](#)]
38. Bao, S.; Wang, Q.; Bian, J. Indoor frost heaving experiment of saline soil in Da'an area, Jilin Province. *J. Eng. Geol.* **2018**, *26*, 1701–1707. [[CrossRef](#)]
39. Konrad, J.M.; Morgenstern, N.R. Effects of applied pressure on freezing soils. *Can. Geotech. J.* **1982**, *19*, 494–505. [[CrossRef](#)]

40. Takashi, T.; Masuda, M.; Yamamoto, H. Experimental study on the influence of freezing speed upon frost heave of soil under constant effective stress. *J. Jpn. Soc. Snow Ice* **1974**, *36*, 49–68. [[CrossRef](#)]
41. Jia, L.; Hou, Z.; Wang, W. Swelling mechanism and restraining measures of sulphate salty soil under freeze-thawing condition. *J. Anhui Agric. Sci.* **2009**, *37*, 3330–3331, 3344. [[CrossRef](#)]
42. Gong, L.; Liu, D.; Yang, N.; Wang, Y.; Zhang, Y. Field experimental study on frost heave of subgrade soil in Xige section of Qinghai—Tibet railway. *Subgrade Eng.* **2018**. [[CrossRef](#)]
43. Gong, L.; Liu, D.; Yang, N.; Wang, Y.; Zhang, Y. Comprehensive analysis on frost heave factors of subgrade soil in seasonally frozen ground region. *Hydro-Sci. Eng.* **2019**, 28–34. [[CrossRef](#)]



© 2019 by the authors. Licensee MDPI, Basel, Switzerland. This article is an open access article distributed under the terms and conditions of the Creative Commons Attribution (CC BY) license (<http://creativecommons.org/licenses/by/4.0/>).